ARMA 19–1621

Experimental and Numerical Investigation of the Microscale Failure Mechanism of a Porous Sandstone during Brazilian Tensile Test Conditions

Chen, B., Latham, J.P. and Xiang J.
Department of Earth Science and Engineering, Imperial College London, London, England, UK
Bakker, R.R.
Delft University of Technology, Delft, Netherlands

ABSTRACT: Rock failure is normally simulated with the mesoscale or macroscale model and the corresponding damage or fracture model based on laboratory scale intact strength parameters. The mesoscale or macroscale model predicts the rock failure plausibly in mesoscale or macro scale problems but may fail in some specific failure mechanisms where the microstructure is believed to play an important role. As an initial step of investigating the complex failure mechanism of sandstone in the context of water jet drilling, the microstructure model of the sandstone was constructed based on CT-scan data in this work and the corresponding failure mechanism during Brazilian tensile test was analyzed. A novel CT-scan based approach is proposed to mimic sandstone microstructure in the numerical model and a compromise between the accuracy of the microstructure model and the computation cost is reached. The microstructure model is solved with the FEMDEM. The capacity of the proposed model in simulating microscale failure of sandstone is well proved in numerical cases.

1. INTRODUCTION

Mesoscale or macroscale model along with the corresponding damage or fracture model has been extensively used for solving rock mechanics problems. However, when it comes to the cases where the microscale failure needs to be focused, the macroscale model no longer satisfies the demand. For example, in the context of water jet drilling, the sandstone grains are flushed from the rock mass by the water jet which has a diameter of only 2mm. Thus, the investigation of microscale rock failure is significant to understand the macroscale response of the rock in specific scenarios, like water jet drilling.

The rock microstructure has been considered in numerical simulation via different kinds of approaches. The simplest approach is to generate the numerical mesh firstly and to assign the phase type and properties to the mesh elements according to specific stochastic distribution or artificially (Mahabadi et al., 2014). Alternatively, a Voronoi diagram might be generated firstly and then the Voronoi polygons are assigned with different type of phase to present the interaction between rock grains (Gao and Kang, 2017; Ghazvinian et al., 2014; J. Li et al., 2017; X. F. Li et al., 2017). The numerical mesh is got through refining the Voronoi polygons. However, in both the two approaches, the component ratio or porosity could be easily satisfied but the pattern for the distribution of different component is completely missing. Another approach is to project the actual mineral distribution from digital image (scanning electron microscope (SEM) or computed tomography (CT)) onto the numerical model which could be consisted of particles, structured or unstructured mesh (Chen et al., 2004, 2006; Lesueur et al., 2017; Li et al., 2019; Mahabadi et al., 2014; Suchorzewski et al., 2018; Yu et al., 2018; Zhao et al., 2014; Zhu et al., 2018). The drawback here is that a smooth boundary between different minerals or grains may become zig-zag after projection and unnecessary fine mesh inside the same kind of minerals or each grain increases the computation cost. Li et al. (2016) reproduced the boundary between rock and soil in the soil-rock mixture with B-splines based on the 2D slice of CT-scan data. But the capacity of presenting complex geometry might be limited. Therefore, how to incorporate the actual complex rock microstructure into the numerical model reasonably with the practical computation cost even in 2D is still a challengeable problem.

The numerical approaches which have been used for solving the deformation or failure of rock microstructure model includes finite element method (FEM) (Li et al., 2019), discrete element method (DEM) (Gao et al., 2016; Peng et al., 2017), finite discrete element method

(FEMDEM) (Abdelaziz et al., 2018; Tatone and Grasselli, 2015). FEM is preferred for deformation analysis without failure considering the high efficiency. But DEM and FEMDEM have the advantage over FEM in the following two aspects. Firstly, the nucleation of the microcracks is relatively easily simulated, which is suitable for simulating rock failure (Lisjak et al., 2018; Ma et al., 2017). Another is that different types of element boundaries between minerals or grains need to be assigned different bonding strength in the microstructure model according to grain-based model (GBM) (Potyondy, 2010), which could be easily implemented in the framework of DEM and FEMDEM once the elements for different minerals and grains are well defined.

The purpose of this paper is to investigate the microscale failure mechanism of a porous sandstone in Brazilian test. The actual sandstone microstructure is presented as far as possible via a novel CT scan-based approach for sandstone microstructure model construction and FEMDEM is adopted to simulate the microscale mechanical behaviors of the sandstone during Brazilian test. The paper is organized as follows. In Section 2, a novel CT scan-based approach for sandstone microstructure model construction is introduced. The FEMDEM concept is briefly summarized in Section 3 and related parameters are calibrated with the experimental results in Section 4. The corresponding results and failure mechanism during the Brazilian test are discussed in Section 5. Finally, some conclusions are presented in Section 6.

2. CT-SCAN BASED CONSTRUCTION OF SANDSTONE MICROSTRUCTURE MODEL

The application of CT-scan data for rock cores and related techniques (i.e. digital rock) initially focus on the pore network recognition and permeability analysis. Conversely, the recognition of the mineral grains and the corresponding topological structure are focused here for mechanical analysis. A novel CT-scan based workflow for constructing sandstone microstructure model was adopted in this section to mimic exactly the sandstone microstructure in the numerical simulation. Firstly, the sandstone microstructure geometry presented by 3D surface mesh was generated within Avizo software (version 9.2) based on the CT-scan data. Then the 2D numerical mesh for sandstone microstructure model on a specific plane could be extracted directly from the 3D surface mesh while the 3D tetrahedra mesh was generated based on the 3D surface mesh.

2.1. Acquisition of CT-scan data

Samples were imaged in 3D using a Phoenix NANOTOM high resolution micro CT (computed tomography) scanner, located in the Geoscience Laboratory at TU Delft. The scanner uses an x-ray-source with maximum voltage of 180 kV, maximum power of 15 W and minimum focal spot size is ~ 0.9 µm. The resolution depends on the sample size and can be as low as 1 µm for a sample size of 1 mm^3. Samples were scanned to a voxel (pixel cube) size of 8 µm. Raw images were corrected for beam hardening effects.

2.2. Construction of Sandstone Microstructure Model

Fig. 1. Construction of sandstone microstructure model in Avizo software: original CT-scan data (top), material segmentation (middle) and particle separation and surface generation (bottom).

The construction of the sandstone microstructure model is done in Avizo software through a series of treatments including material segmentation, grain separation, surface generation, etc., as shown in Figure 1. The main processes are briefly described here. Firstly, a median filter is applied to the CT-scan data to avoid noises. Then interactive thresholding is adopted to segment the sandstone grains and pore. Afterwards, the sandstone grains are recognized and separated with each other using watershed segmentation technique. The grain surfaces are then generated using the Surface Generation tool and are presented by the triangle mesh generated directly from the voxels.

2.3. *Extraction of 2D Numerical Mesh*

The 2D numerical mesh for sandstone microstructure model can be extracted from the 3D surface mesh generated in Section 2.2 on a specific plane. The information for the 2D numerical model is written into a mesh file for GID (a pre-processing software) input. An example of the 2D numerical microstructure model is shown in Figure 2.

Fig. 2. An example of the 2D numerical microstructure model with a diameter of 10mm.

3. CONCEPTS OF FEMDEM MODEL

FEMDEM is adopted in our simulation and the corresponding theory has been described in detail by Xiang et al. (2009). FEMDEM is capable of simulating the transient process from the continuum body to dis-continuum body, which makes it a suitable numerical method for rock failure simulation. The deformation of each dis-continuum body is solved with FEM while the contact between different dis-continuum bodies is solved with DEM concepts. The numerical parameters including elastic modulus, Poisson ratio, tensile strength, energy release rate, etc. are determined according to the experimental results in Sect. 4.

4. CALIBRATION OF THE NUMERICAL MODEL WITH EXPERIMENTAL RESULTS

In order to determine the key parameters in the FEMDEM model, the numerical model is calibrated with the experimental Brazilian test results in this section. The input parameters for the numerical model include: 1) parameters for elements, density ρ, elastic modulus E and Poisson's ratio, v; 2) parameters for the elastic interaction between elements, elastic penalty, k_n, contact penalty k_c; 3) parameters related to the fracture model for element boundaries, tensile strength f_t, internal friction coefficient k_μ, internal cohesion c, Mode I and Mode II fracture energy release rate G_I and G_{II}; 4) mass damping coefficient μ. The experimental results are reported firstly and then the details about the numerical set-up are given and the model is calibrated with the experimental results.

4.1. *Experimental Set-up and Results*

The geometries and the test results of the six Bentheim sandstone samples are listed in Table 1. A relatively small sample size is used here considering the influence of the microstructure is believed to play a more important role in a smaller scale. The samples are tested using an in-house developed stiff loading frame as installed at the TU Delft rock mechanics laboratory, designed to handle a maximum load of 50 kN without significant apparatus compliance. Samples were deformed at a constant velocity of 20 µm/s, leading to sample failure on a relatively short timescale as per ASTM standards. Load control was avoided such that the microstructure could be preserved. Diametral (line) load was measured with a load cell to an accuracy of 0.01 kN. Displacement was calculated by the average of two co-axially mounted Linear Variable Differential Transducers (LVDT) with an accuracy of 1 µm. Data was logged at 10 Hz such that ample data is available to allow precise comparison with numerically derived data. The loading force-displacement curves are shown in Figure 3 and vary considerably between different samples (1.6–3.2 MPa in indirect tensile strength) due to microscale heterogeneities and/or imperfections in sample dimensions from preparations. Individual measurement errors fall within the line thicknesses.

Table 1 Geometries and test results of the six Bentheim sandstone samples

Sample	A	B	C	D	E	F
Diameter (mm)	10.00	10.05	10.10	10.00	10.05	10.10
Thickness (mm)	6.85	5.45	5.70	4.90	6.00	5.60
Peak loading (kN)	0.337	0.328	0.233	0.228	0.175	0.229
Indirect tensile strength (MPa)	3.133	3.044	2.166	2.115	1.626	2.131

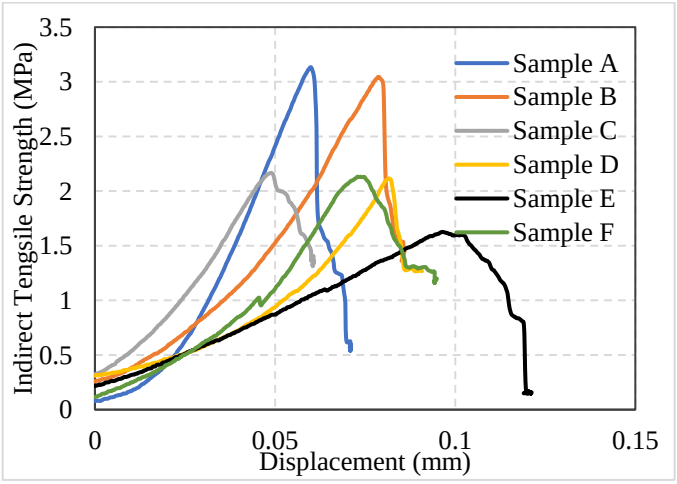

Fig. 3. Brazilian test results of the Bentheim sandstone samples.

4.2. Numerical Set-up

The numerical model set-up is shown in Figure 4. The two loading platens were placed close to the specimen with no gap and were both assigned a constant velocity of 0.01m/s towards the specimen. Although the resultant loading velocity was much higher than that used in the experiment, the reasonability of the boundary condition has been well proved in literatures. A sensitivity study of the loading velocity has also been conducted before the calibration. According to the theory of FEMDEM model, the time step should satisfy:

$$\Delta t < \sqrt{\frac{V_{\min}\rho}{\max(E, k_n, k_c)}} \quad (1)$$

where $V_{\min}$ is the minimum element volume in the simulation, ρ is the density, E, k_n and k_c are the elastic modulus, elastic penalty and contact penalty respectively.

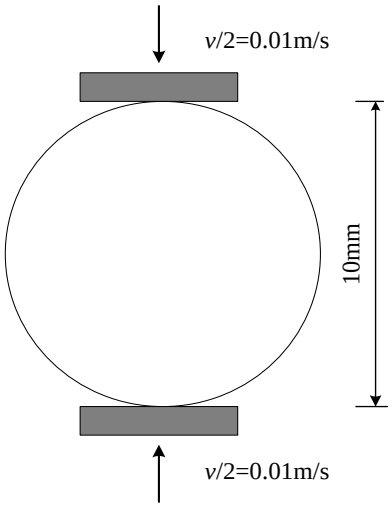

Fig. 4 Numerical model set-up of Brazilian test.

The 2D numerical microstructure model constructed from the CT-scan data of the Brazilian test sample A is used in the simulation and the 2D slice was taken from the middle of the sample. In order to reduce the high computation cost during the calibration, a disc with a half diameter of the original sample was taken and was enlarged twice. The microstructure model has 8,960 triangular elements and a nominal element size of 0.06 mm.

4.3. Determination of the Numerical Parameters

The numerical parameters in the microstructure numerical model are calibrated with the experimental results in this section. The bulk density, Young's modulus, Poisson's ratio, cohesion and internal friction coefficient were obtained through other experimental tests. According to the data from Perras and Diederichs (2014), the ratio of the tensile strength tested from direct tensile to the indirect tensile strength from Brazilian test for sandstone is around 2. Therefore, the tensile strength used in the simulation was fixed at 1.19MPa, half of the average indirect tensile strength from experiments 2.37MPa. The elastic and contact penalty number are determined to be 20 and 10 times of Young's modulus. The Mode I and Mode II energy release rate GI and GII were adjusted to match the numerical result with the averaged indirect tensile strength value. The final parameters used in the simulation are listed in Table 2.

Table 2 Input parameters of the 2D microscale simulation for Brazilian test calibrated with experimental results

Element properties	**Values**
Bulk density, ρ(kg/m^3)	2,700
Young's modulus, E(GPa)	17.00
Poisson's ratio, v	0.14
Tensile strength, f_t(MPa)	1.19
Cohesion, c(MPa)	8.00
Internal friction coefficient, k_μ	0.60
Mode I energy release rate, G_I(J/m^2)	5.5
Mode II energy release rate, G_{II}(J/m^2)	100.00
Elastic penalty, k_n(GPa)	340.00
Contact penalty, k_c(GPa)	170.00

5. RESULTS AND DISCUSSION

With the numerical set-up and parameters in Section 4, the numerical results are obtained and discussed in this section. The resultant displacement-force curve from the simulation is drawn in Figure 5 and the evolution of the generated crack is shown in Figure 6.

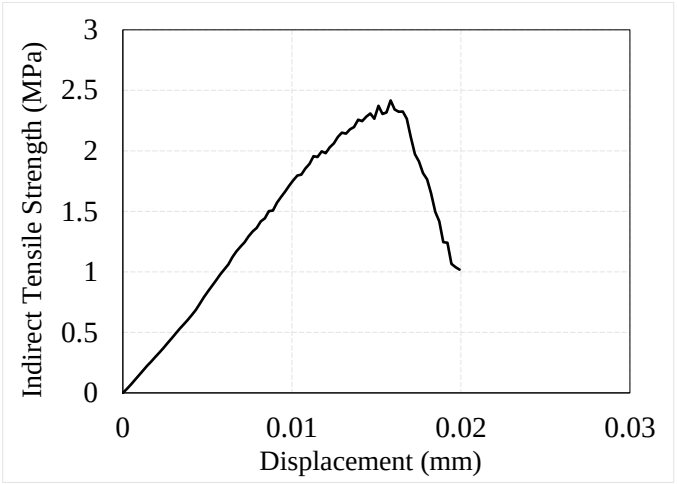

Fig. 5. Displacement-force curve from numerical simulation.

As shown in Figure 5, a nearly linear increase of the loading force was observed, which is similar as the results in literatures (Tatone and Grasselli, 2015), but is different from the curve in the experiment due to the lack of simulation of grain interaction and compression of pores at the initial stage. Comparing these initial numerical results with laboratory data shows that in terms of tensile strength results are comparable. However, in terms of displacement, the numerical data is much less than the laboratory data. It is because that much displacement was consumed due to the close of the possible gap between grains, pore compression and the adjustment between sample and platens in the beginning stage of the

experiment. The evolution of the generated crack is shown in Figure 6. A vertical crack generated from the center of the sample and crossed several pores and developed into a main crack eventually.

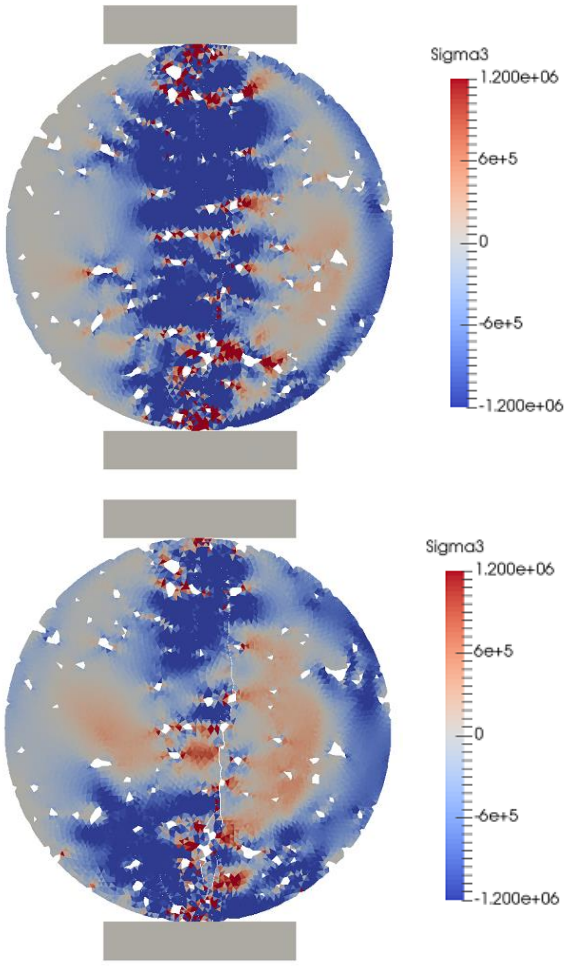

Fig. 6. Generated crack during numerical Brazilian test: crack initiation (top) and propagation (bottom).

As an initial study, the current study is still restricted in the following two aspects. Due to the high computation cost during calibration, a relatively small 2D model was used in our simulation. A 3D model with 1:1 size microstructure is expected to simulate the failure of sandstone sample during Brazilian test more accurately. Another thing is that the interaction between inter-grain and intra-grain elements are simulated with the same properties, which does not describe the microscale interaction between sandstone grains in the real case. A more advanced model is under development.

6. CONCLUSIONS

In this paper, the influence of the microscale structure on the failure mechanism of a porous sandstone is investigated in the context of the Brazilian test. The main contributions are summarized on the following two aspects.

A novel approach for constructing the rock microstructure model based on CT-scan data is implemented. Different from the existing approaches where the mineral types are assigned to the pre-generated mesh artificially or according to specific stochastic distribution, our approach started from the real CT-scan data and constructed the geometry and then generated the numerical mesh to target a numerical mimic of the actual rock microstructure. The rock microstructure presented with millions of voxels in original CT-scan data were represented with two orders of magnitude fewer number of unstructured triangles. A compromise between the accuracy of the microstructure model and the element numbers (roughly proportional to the computation cost of the numerical model) used was reached. The actual microstructure information was kept from the CT-scan data as much as possible under a specific limitation of computation cost.

With the microstructure model constructed, the influence of the microstructure on the failure mechanism of a porous sandstone during the Brazilian tensile test was investigated with FEMDEM model. The numerical parameters in the FEMDEM model were calibrated with the experimental results. A vertical crack generated from the center of the sample and crossed several pores and developed into a main crack eventually. The significant influence of the pores is well verified in the simulation.

ACKNOWLEGMENTS

This project has received funding from the European Union's Horizon 2020 research and innovation programme under grant agreement No. 654662.

REFERENCES

1. Abdelaziz, A., Q. Zhao, and G. Grasselli. 2018. Grain based modelling of rocks using the combined finite-discrete element method. *Computers and Geotechnics, 103*, 73-81.
2. Chen, S., Z. Q. Yue, and L. G. Tham. 2004. Digital image-based numerical modeling method for prediction of inhomogeneous rock failure. *International Journal of Rock Mechanics and Mining Sciences, 41*(6), 939-957.
3. Chen, S., Z. Q. Yue, and L. G. Tham. 2006. Digital Image Based Approach for Three-Dimensional Mechanical Analysis of Heterogeneous Rocks. *Rock Mechanics and Rock Engineering, 40*(2), 145-168.
4. Gao, F., and H. Kang. 2017. Grain-Based Discrete-Element Modeling Study on the Effects of Cementation on the Mechanical Behavior of Low-Porosity Brittle Rocks. *International Journal of Geomechanics, 17*(9), 04017061.
5. Gao, F., D. Stead, and D. Elmo. 2016. Numerical simulation of microstructure of brittle rock using a grain-breakable distinct element grain-based model. *Computers and Geotechnics, 78*, 203-217.
6. Ghazvinian, E., M. S. Diederichs, and R. Quey. 2014. 3D random Voronoi grain-based models for simulation of

brittle rock damage and fabric-guided micro-fracturing. *Journal of Rock Mechanics and Geotechnical Engineering, 6*(6), 506-521.
7. Gui, Y. L., Z. Y. Zhao, J. Ji, X. M. Wang, K. P. Zhou, and S. Q. Ma. 2016. The grain effect of intact rock modelling using discrete element method with Voronoi grains. *Géotechnique Letters*, 6(2), 136-143.
8. Lesueur, M., M. C. Casadiego, M. Veveakis, and T. Poulet. 2017. Modelling fluid-microstructure interaction on elasto-visco-plastic digital rocks. *Geomechanics for Energy and the Environment, 12*, 1-13.
9. Li, C.-S., D. Zhang, S.-S. Du, and B. Shi. 2016. Computed tomography based numerical simulation for triaxial test of soil–rock mixture. *Computers and Geotechnics, 73*, 179-188.
10. Li, J., H. Konietzky, and T. Frühwirt. 2017. Voronoi-Based DEM Simulation Approach for Sandstone Considering Grain Structure and Pore Size. *Rock Mechanics and Rock Engineering, 50*(10), 2749-2761.
11. Li, X., Z. Liu, S. Cui, C. Luo, C. Li, and Z. Zhuang. 2019. Predicting the effective mechanical property of heterogeneous materials by image based modeling and deep learning. *Computer Methods in Applied Mechanics and Engineering, 347*, 735-753.
12. Li, X. F., H. B. Li, and J. Zhao. 2017. 3D polycrystalline discrete element method (3PDEM) for simulation of crack initiation and propagation in granular rock. *Computers and Geotechnics, 90*, 96-112.
13. Lisjak, A., O. K. Mahabadi, L. He, B. S. A. Tatone, P. Kaifosh, S. A. Haque, and G. Grasselli. 2018. Acceleration of a 2D/3D finite-discrete element code for geomechanical simulations using General Purpose GPU computing. *Computers and Geotechnics, 100*, 84-96.
14. Liu, Q., Y. Jiang, Z. Wu, and J. He. 2018. A Voronoi element based-numerical manifold method (VE-NMM) for investigating micro/macro-mechanical properties of intact rocks. Engineering Fracture Mechanics, 199, 71-85.
15. Ma, G., W. Zhou, R. A. Regueiro, Q. Wang, and X. Chang. 2017. Modeling the fragmentation of rock grains using computed tomography and combined FEMDEM. *Powder Technology, 308*, 388-397.
16. Mahabadi, O. K., B. S. A. Tatone, and G. Grasselli. 2014. Influence of microscale heterogeneity and microstructure on the tensile behavior of crystalline rocks. *Journal of Geophysical Research: Solid Earth, 119*(7), 5324-5341.
17. Peng, J., L. N. Y. Wong, and C. I. Teh. 2017. Influence of grain size heterogeneity on strength and microcracking behavior of crystalline rocks. *Journal of Geophysical Research: Solid Earth, 122*(2), 1054-1073.
18. Perras, M. A., and M. S. Diederichs. 2014. A Review of the Tensile Strength of Rock: Concepts and Testing. *Geotechnical and Geological Engineering*, 32(2), 525-546.
19. Potyondy, D. O. (2010, June 9-12, 2010). *A Grain-Based Model for Rock: Approaching the True Microstructure*. Paper presented at the Rock Mechanics in the Nordic Countries 2010, Kongsberg, Norway.
20. Suchorzewski, J., J. Tejchman, and M. Nitka. 2018. Experimental and numerical investigations of concrete behaviour at meso-level during quasi-static splitting tension. *Theoretical and Applied Fracture Mechanics, 96*, 720-739.
21. Tatone, B. S. A., and G. Grasselli. 2015. A calibration procedure for two-dimensional laboratory-scale hybrid finite–discrete element simulations. *International Journal of Rock Mechanics and Mining Sciences, 75*, 56-72.
22. Xiang, J., A. Munjiza, and J.-P. Latham, 2009, Finite strain, finite rotation quadratic tetrahedral element for the combined finite–discrete element method. *International Journal for Numerical Methods in Engineering*, 79(8):946–978.
23. Yu, Q., H. Liu, T. Yang, and H. Liu. 2018. 3D numerical study on fracture process of concrete with different ITZ properties using X-ray computerized tomography. *International Journal of Solids and Structures, 147*, 204-222.
24. Zhao, G.-F., A. R. Russell, X. Zhao, and N. Khalili. 2014. Strain rate dependency of uniaxial tensile strength in Gosford sandstone by the Distinct Lattice Spring Model with X-ray micro CT. *International Journal of Solids and Structures, 51*(7-8), 1587-1600.
25. Zhu, J. B., T. Zhou, Z. Y. Liao, L. Sun, X. B. Li, and R. Chen. 2018. Replication of internal defects and investigation of mechanical and fracture behaviour of rock using 3D printing and 3D numerical methods in combination with X-ray computerized tomography. *International Journal of Rock Mechanics and Mining Sciences, 106*, 198-212.